Journal of Solid State Chemistry 184 (2011) 905–910

Contents lists available at ScienceDirect

Journal of Solid State Chemistry

journal homepage: www.elsevier.com/locate/jssc

Phonons in isostructural (ND,Yb):$Y_xGd_{1-x}(VO_4)$ laser crystals: A Raman scattering study

Nana Zhang [a,b], Jiyang Wang [a,**], Xiaobo Hu [a], Huaijin Zhang [a], C.C. Santos [c], A.P. Ayala [b], I. Guedes [b,*]

[a] State Key Laboratory of Crystal Materials, Shandong University, Jinan 250100, PR China
[b] Departamento de Física, Universidade Federal do Ceará, Campus do Pici, CP 6030, Fortaleza CE 60455-760, Brazil
[c] Departamento de Física, CCET, Universidade Federal do Maranhão, 65085-580 São Luis, MA, Brazil

ARTICLE INFO

Article history:
Received 11 November 2010
Received in revised form
11 February 2011
Accepted 20 February 2011
Available online 26 February 2011

Keywords:
Raman spectra
Zircon structure
One-phonon behavior
Laser crystals

ABSTRACT

The room temperature phonon modes of the isostructural (Nd,Yb):$Y_xGd_{1-x}(VO_4)$ laser crystals were determined using the Raman scattering technique, and the observed wavenumbers follow the overall mode distribution expected for $REVO_4$ (RE=rare earth) compounds with the tetragonal zircon structure, D_{4h}^{19}. They were assigned according to the group theory in terms of the internal modes of the VO_4 tetrahedron and the external modes of the $Y_xGd_{1-x}(VO_4)$ lattice. No appreciable changes in the phonon wavenumbers were observed for Yb:$GdVO_4$ (Yb=0.008, 0.015, 0.020, 0.025, and 0.035), indicating that the force fields in the $GdVO_4$ lattice are not strongly altered by Yb doping at the Gd site. However, most of the phonon wavenumbers in the systems (Nd,Yb):$Y_xGd_{1-x}(VO_4)$ shifts upwards (one-phonon-like behavior) when Y replaces for Gd.

1. Introduction

The $REVO_4$ series of compositions (RE=Pr to Lu including Sc and Y) exhibits the tetragonal (zircon-type) D_{4h}^{19} structure with four molecules per unit cell (Z=4). Among several other applications, these compounds have been used as laser hosts due to their good optical quality and high chemical durability. For instance, a large number of papers demonstrating laser action in the systems Nd:YVO_4 and Nd:$GdVO_4$ have already been published [1–9]. Since Nd:YVO_4 and Nd:$GdVO_4$ crystals are isostructural and have similar melting point, it is possible to obtain an infinite soluble Nd:$Y_xGd_{1-x}VO_4$ solution and grow crystals with good optical quality.

The mixed crystals have attracted an increasing interest due to their potential application for high pump power pulsed lasers. Moreover, laser action in either continuous-wave (cw) or pulsed mode has been demonstrated. In 2010, Liu et al. [10] reported on the actively Q-switched laser performance of the Nd:$Y_xGd_{1-x}VO_4$ crystals. Liu et al. [11] also reported on the cw laser performance of the $Yb_{0.009}$:$Y_{0.575}Gd_{0.416}VO_4$ crystal. Ng et al. [12] demonstrated a passively Q-switched Nd:$Gd_{0.64}Y_{0.36}VO_4$ laser with a Cr^{4+}:YAG saturable absorber. He et al. [13] demonstrated a passively mode-locked Nd:$Gd_{0.5}Y_{0.5}VO_4$ laser with a semiconductor saturable absorber mirror. Liu et al. [14] discussed the improvement of passive Q-switching performance of Nd:$Gd_{0.64}Y_{0.36}VO_4$ as compared to that of Nd:YVO_4 and Nd:$GdVO_4$. Zhang et al. [6] demonstrated laser performance at 1.34 μm for Nd:$Gd_{0.8}La_{0.2}VO_4$. Yu et al. [15] demonstrated cw laser performance at 1.06 μm for Nd:$Lu_xGd_{1-x}VO_4$ pumped by a diode laser.

Because of the tightly bound VO_4 tetrahedra in $REVO_4$, a simplified structure can be considered as being composed of two sublattices of RE and VO_4 “molecules”, with both RE and VO_4 occupying the crystallographic sites D_{2d}. For a $REVO_4$ crystal with zircon-type structure, the first-order Raman phonon spectrum consists of narrow lines that correspond to Raman-allowed zone-center modes, which obey definite polarization selection rules.

Room-temperature Raman phonons of some of the $REVO_4$ compounds have been reported previously. Polarized results can be found for $PrVO_4$ [16], $NdVO_4$ [16], $GdVO_4$ [17], $TbVO_4$ [17], $DyVO_4$ [17], and $ErVO_4$ [18], while unpolarized results can be found for $TmVO_4$ [19], $LaVO_4$ [20], $CeVO_4$ [21], $SmVO_4$ [22], $EuVO_4$ [19], $HoVO_4$ [23], $YbVO_4$ [19], and $LuVO_4$ [23]. Recently, Santos et al. [24] provided a more accurate description of the room-temperature phonons for $SmVO_4$, $HoVO_4$, $YbVO_4$, and $LuVO_4$ single crystals. Of the 12 zone-center Raman phonons expected, they observed 10 phonons for $SmVO_4$ and $HoVO_4$ and 9 for $YbVO_4$ and $LuVO_4$. The phonon symmetry assignment was given based on correlations with previous results for other $REVO_4$ compounds. Also, they analyzed the correlation among the observed Raman wavenumbers and the rare earth atomic number

---

[*] Corresponding author. Fax: +55 85 3366 9450.
[**] Corresponding author. Fax: +86 531 88366423.
E-mail addresses: jywang@sdu.edu.cn (J. Wang), guedes@fisica.ufc.br (I. Guedes).

0022-4596/$ - see front matter © 2011 Elsevier Inc. All rights reserved.
doi:10.1016/j.jssc.2011.02.018

(Z) in order to determine the extent of the variation as RE increases in Z along the lanthanide series.

For a mixed $RE'_xRE''_{1-x}(VO_4)$ crystal the following features may be observed from the phonon spectrum: (i) a broadening of the first-order Raman lines; (ii) activation of forbidden Raman phonons; (iii) appearance of broad Raman bands reflecting the phonon density of states; (iv) wavenumber shifting of some peaks proportional to the concentration of the dopant element (i.e., one-phonon-like behavior), and (v) splitting of some peaks involving different elements that share the same lattice site (i.e., two-phonon-like behavior).

In the present work, we use Raman spectroscopy to investigate the extent of the modification of the $GdVO_4$ phonons due to the doping of the Gd site by Y, Yb, and Nd. We observed that the wavenumber of most of the vibrations increases when Y replaces for Gd in the (Nd,Yb):$Y_xGd_{1-x}(VO_4)$ crystals, while it remains approximately constant when Yb replaces for Gd in the Yb:Gd(VO_4) crystal. Besides providing information about the disorder on the zircon structure as x increases, Raman spectroscopy yields information about the maximum phonon energy, used in the analysis of loss mechanism of a given electronic transition (lifetime).

2. Experimental

Single crystals of (Nd,Yb):$Y_xGd_{1-x}(VO_4)$ were prepared following the procedure described elsewhere [25–27]. The concentrations of Nd^{3+}, Gd^{3+}, Y^{3+}, and Yb^{3+} ions were measured by the X-ray fluorescence (XRF) analysis method. The crystal structures were measured using an X-ray powder diffractometer (XRPD) (Bruker, model: Smart PPEX II) with Cu$K\alpha 1$ line ($\lambda = 1.5406 \times 10^{-10}$ m). We observed that all as-grown (Nd,Yb):$Y_xGd_{1-x}(VO_4)$ crystals possess the tetragonal (zircon-type) structure belonging to the D_{4h}^{19} space group. Backscattered polarized Raman spectra were recorded on a Jobin–Yvon Model T64000 triple spectrometer with a spectral resolution of 2 cm^{-1}. The instrument was equipped with a liquid-N_2-cooled charge-coupled device system. For spectral excitation, green 514.5 nm radiation from a Coherent Model Innova 70 Ar^+-ion laser operating at

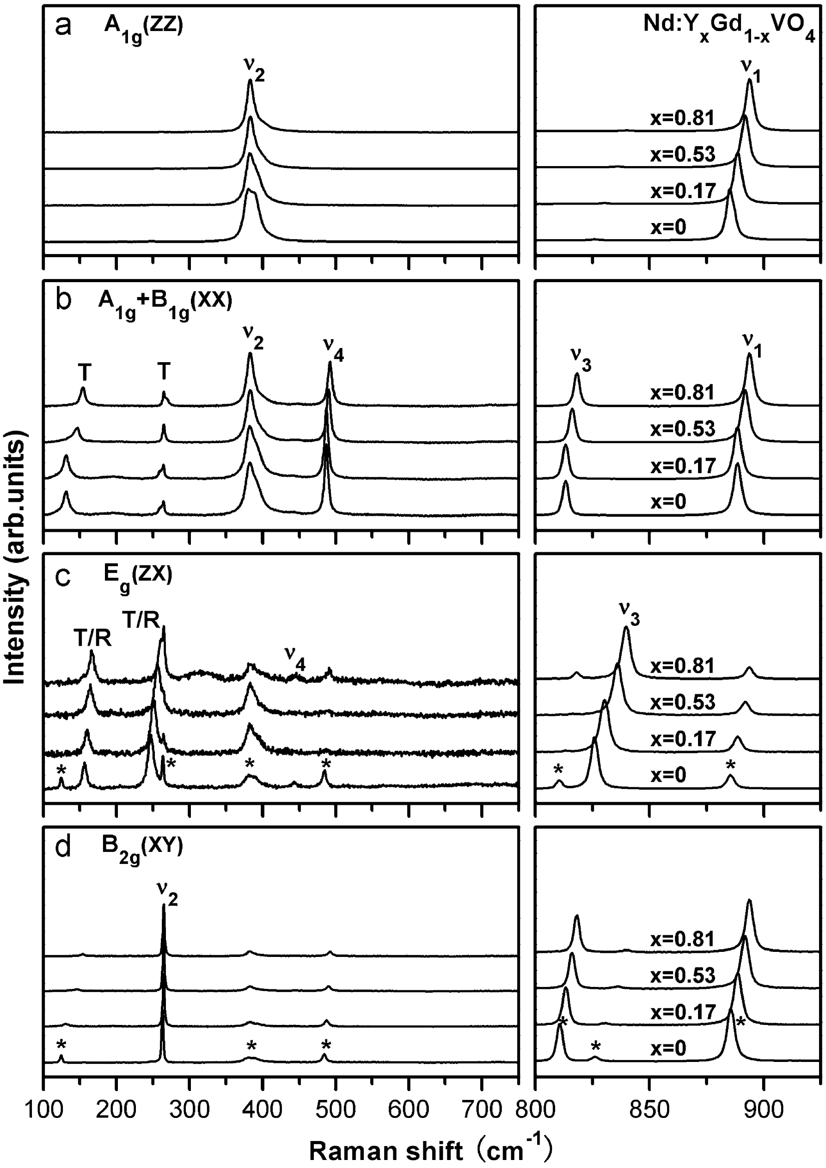

Fig. 1. Room temperature polarized Raman spectrum of Nd:$Y_xGd_{1-x}VO_4$ (x=0.0, 0.17, 0.53, and 0.81), recorded in different polarizations: (a) (zz), (b) (xx), (c) (zx), and (d) (xy).

30 mW was employed. Scattering geometries for the spectra listed in the text, tables and figures follow the usual Porto's notation [28].

The typical crystal selected for the Raman study consisted of a parallelepiped, whose average dimensions were $6\times6\times2$ mm^3. They form three families of rare-earth vanadates, namely: (i) yNd:$Y_xGd_{1-x}(VO_4)$, where $y=0.005$ and $x=0.0$, 0.17, 0.37, 0.53, 0.63, 0.7, 0.81, and 1.0; (ii) yYb:Gd(VO_4), where $y=0.008$, 0.015, 0.020, 0.025, and 0.035; and (iii) yYb:$Y_xGd_{1-x}(VO_4)$, where $(y,x)=(0.0135, 0.87)$, (0.0118, 0.74), (0.0092, 0.58), (0.0071, 0.41) and (0.0048, 0.3).

3. Results and discussion

Kolitsch and Holstam [29], showed that the $REVO_4$ ($RE=$Nd, Yb, Y, and Gd) are isostructural, exhibiting a tetragonal (zircon-type) structure belonging to D_{4h}^{19} space group with four molecules per unit cell ($Z=4$), where RE and VO_4 occupy D_{2d} crystallographic sites. In Ref. [30], Isasi et al. showed that in the mixed $Y_xGd_{1-x}(VO_4)$, the rare-earths Y and Gd share the same D_{2d} crystallographic site.

By considering that the zircon structure is composed of two sublattices of RE^{3+} (or RE'/RE'') ions and VO_4^{3-} "molecules", and using the group theory analysis the Raman-active modes can be decomposed in terms of the irreducible representations of the D_{4h} point group as $\Gamma=A_{1g}(\nu_1,\nu_2)+B_{1g}(2T,\nu_3,\nu_4)+B_{2g}(\nu_2)+E_g(2T,R,\nu_3,\nu_4)$, where ν_i $(i=1,\ldots,4)$ correspond to the internal modes of the VO_4 tetrahedron, and T/R corresponds, respectively, to the translational (T) or rotational (R) motion involving both the RE and VO_4 ions.

Fig. 1(a)–(d) show the room temperature Raman spectra of Nd:$Y_xGd_{1-x}(VO_4)$ for (zz), (xx), (zx) and (xy) polarizations, respectively. These polarizations yield the Raman modes of A_{1g}, $A_{1g}+B_{1g}$, E_g, and B_{2g} symmetry, respectively. For $x=0.0$, Fig. 1(a) shows the two A_{1g} modes predicted by the group theory analysis. They correspond to the symmetric bending (ν_2) at 379 cm^{-1} and the symmetric stretching (ν_1) at 885 cm^{-1}.

It should be noted that the $A_{1g}(\nu_2)$ vibration mode exhibits an inhomogeneous splitting ($\Delta\sim11$ cm^{-1}) similar to those observed in Ref. [31] for Nd:$GdVO_4$. This splitting has been observed even for pure $GdVO_4$ [32]. Let A and B be the low- and high-frequency components of the $A_{1g}(\nu_2)$ doublet with integrated intensities I_A and I_B, respectively. As x increases Δ and I_B/I_A decrease.

In Ref. [32] the splitting of the $A_{1g}(\nu_2)$ mode over a wide temperature range 14–800 K was investigated. The splitting observed was associated with the thermally activated process of disorientation of the VO_4 groups in the zircon structure.

Similar splitting was observed for $TbVO_4$ when P replaces for V [33]. For pure $TbVO_4$ the structure has an exact translational symmetry and no splitting of the $A_{1g}(\nu_2)$ is observed, indicating that the VO_4 tetrahedra are well oriented. However, for mixed $Tb(V_{1-x}P_x)O_4$ crystals the local structure could *a priori* differ from the average tetragonal structure due to the random distribution of VO_4 and PO_4 groups in the D_{2d} sites. So, while the Tb sublattice retains a good approximation, its translational symmetry, the (V, P)O_4 sublattice does not. In either case, the disorder in the distribution of VO_4 tetrahedra leads to the appearance of the $A_{1g}(\nu_2)$ doublet observed for some rare-earth orthovanadates.

Fig. 1(b) shows, in addition to the A_{1g} modes, the four B_{1g} modes expected. We assign the asymmetric stretching (ν_3) mode at 810 cm^{-1} and the asymmetric bending (ν_4) at 485 cm^{-1}. The modes at 125 and 263 cm^{-1} are related to T-like vibrations. Of the five expected E_g modes, we observe (Fig. 1(c)) four modes at 156, 247, 443, and 826 cm^{-1}. The modes at 443 and 826 cm^{-1} are assigned as ν_4 and ν_3 vibrations, respectively. The remaining two modes at 156 and 247 cm^{-1} are likely to involve R- and/or T-like motions of the atoms. In Fig. 1(d) we observe an intense vibration at 263 cm^{-1} corresponding to the ν_2 mode with B_{2g} symmetry. We recall that, according to Ref. [34], the modes $R(E_g)$, $T(B_{1g})$, and $\nu_2(B_{2g})$ have similar wavenumbers. The calculated ratio between the wavenumbers corresponding to the $\nu_2(B_{2g})$ and $T(B_{1g})$ modes

Table 1
Wavenumbers (in cm^{-1}) and symmetry assignment of y(Nd,Yb):$Y_xGd_{1-x}(VO_4)$.

Crystal	Content	Internal modes							External modes			
		A_{1g} (ν_1)	E_g (ν_3)	B_{1g} (ν_3)	B_{1g} (ν_4)	E_g (ν_4)	A_{1g} (ν_2)	B_{2g} (ν_2)	B_{1g}	E_g	E_g	B_{1g}
Nd:$Y_xGd_{1-x}VO_4$	$x=0.00$	885	826	810	485	…	379	263	263	247	156	125
	$x=0.17$	888	830	813	487	…	382	265	263	251	160	131
	$x=0.37$	890	833	815	489	…	383	265	264	254	162	138
	$x=0.53$	892	836	816	490	…	383	265	265	256	164	145
	$x=0.63$	892	837	817	491	…	383	265	265	258	165	148
	$x=0.70$	893	838	817	492	…	382	265	265	259	165	150
	$x=0.81$	894	840	818	492	…	383	265	266	262	166	154
	$x=1.00$[a]	895	819	821	492	…	380	264	263	262	166	161
yYb:$GdVO_4$	$y=0.008$	885	826	810	485	443	379	263	263	247	156	125
	$y=0.015$	886	826	811	485	443	379	263	263	247	157	125
	$y=0.020$	886	826	811	485	444	380	263	263	247	157	124
	$y=0.025$	886	827	811	485	444	380	263	263	247	157	124
	$y=0.035$	886	827	811	485	444	380	263	263	248	157	124
yYb:$Y_xGd_{1-x}VO_4$	$y=0.0048$ $x=0.30$	889	832	814	488	…	382	264	264	253	160	135
	$y=0.0071$ $x=0.41$	890	834	814	489	…	382	264	264	254	161	140
	$y=0.0092$ $x=0.58$	891	836	816	490	…	383	264	264	257	163	146
	$y=0.0118$ $x=0.74$	892	838	816	491	…	382	264	264	259	165	151
	$y=0.0135$ $x=0.87$	892	839	817	491	…	382	263	263	261	166	155

[a] Ref. [31].

is 1.03, while from our measurements we have 1.0. The asterisks indicate leakage from other polarizations, since the *RE*VO_4 compounds are known to exhibit a relatively large birefringence (>0.2).

The wavenumbers observed for $x=0.0$ agree with those reported in Refs. [17,32] for $GdVO_4$. The Raman results indicate that the phonon spectra of Nd:$GdVO_4$ exhibits a relatively small alteration, suggesting that the $GdVO_4$ lattice is largely insensitive to Nd doping, at least for a Nd concentration of 0.005. In going from $NdVO_4$ to $GdVO_4$ the wavenumbers of the internal VO_4 modes increases by 1.7% on average [24], while the observed shift for $Nd_{0.005}$:$GdVO_4$ is 0.15%. The wavenumbers observed are listed in Table 1, where we also list the wavenumbers of Nd:YVO_4 [31], which are similar to those of YVO_4 [32,35].

When x goes from 0 to 1, most of these modes shift towards higher wavenumbers. The wavenumber of the internal $\nu_1(A_{1g})$, $\nu_3(E_g)$, $\nu_3(B_{1g})$, and $\nu_2(A_{1g})$ modes, and external E_g (156 and 247 cm^{-1}) and B_{1g} (125 cm^{-1}) modes increase, while that of the external B_{1g} (263 cm^{-1}) mode remains practically constant.

The hardening of the internal mode wavenumbers was first explained as resulting from the *RE* contraction, which would lead to a closer packing of the $(PO_4)^{3-}$ units as one proceeds from monazite-type $LaPO_4$ to zircon-type $LuPO_4$ and a shortening of the P–O distances to yield higher wavenumbers [36]. However, crystallographic studies of the $REPO_4$ series performed by Beall et al. [37], Mullica et al. [38–40], and Ni et al. [41] have shown that the length of the *RE*–O bonds decreases rather than the P–O separation when *Z* increases. Usually, the PO_4 tetrahedra are bonded very tightly, and so it is unlikely that they can be deformed when the crystal is heated or under pressure [42].

Such variations also occur for the *RE*VO_4 compounds, where the V–O distance decreases by 0.2%, while the distance *RE*–O is reduced by 6% on average in proceeding from La to Lu [24]. This implies that the crystal lattice is contracting in a manner that keeps almost constant the size of the VO_4 tetrahedron.

In Ref. [25] it is shown that the crystal lattice of the system $Nd_{0.005}$:$Y_xGd_{1-x}(VO_4)$ contracts when x goes from 0 to 1. In accordance with Refs. [43,44], the *RE*–O distance is reduced by

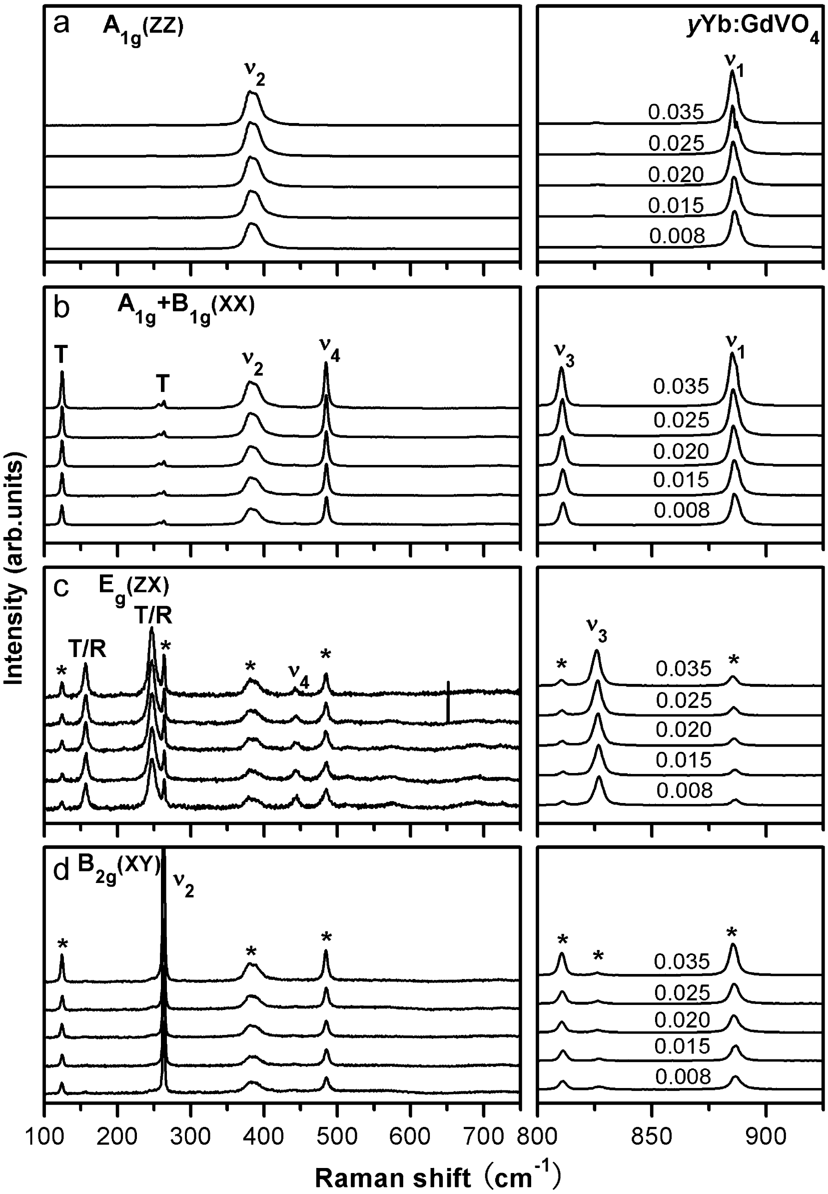

Fig. 2. Room temperature polarized Raman spectra of *y*Yb:$GdVO_4$ (y=0.008, 0.015, 0.020, 0.025, and 0.035), recorded in different polarizations: (a) (*zz*), (b) (*xx*), (c) (*zx*), and (d) (*xy*).

1.7% on average when Y replaces for Gd, while the V–O distances increase by 0.4%. This indicates that the increase in the wavenumber of the internal modes is related to the decrease of the *RE*–O distance due to the lattice contraction, which leads to an increase in the energy of the VO_4 tetrahedron yielding higher stretching and bending wavenumbers [24].

Three out of the four external modes also shift towards higher wavenumbers as *Z* increases. This effect is also related to the overall lattice contraction (~4%) when *x* goes from 0 to 1 [25]. The wavenumber of the B_{1g} mode at ~263 cm^{-1} remains practically constant, since it is primarily associated with the VO_4 motion [33].

Due to the lack of luminescence quenching, larger amounts of Yb^{3+} than Nd^{3+} can be incorporated into $GdVO_4$ lattice for high pump power pulsed lasers. So, we have grown yYb:Gd(VO_4) crystals, with $y=0.008$, 0.015, 0.020, 0.025, and 0.035. Their Raman spectra are shown in Fig. 2(a)–(d). In addition to the modes observed in Fig. 1(a)–(d), we observe a vibration at 444 cm^{-1} which is assigned to the ν_4 mode with E_g symmetry [32]. No changes were observed in the Raman spectra for different Yb^{3+} concentrations, indicating that Yb^{3+} doping produces no significant modification in the zircon-type structure of $GdVO_4$ crystal. The wavenumbers of the Yb:$GdVO_4$ compounds are also listed in Table 1.

This result agrees with those previously reported by Hu et al. [45] who observed from the X-ray powder diffraction technique, that the Yb^{3+} ions do not alter the essential zircon-type structure of $GdVO_4$ even for doping levels as high as 0.17. For $y=0.0646$, the variation of the unit cell volume is only ~0.5%.

Having realized that Yb^{3+} doping at the Gd site does not change the lattice structure, the modification in the Raman spectra of yYb:$Y_xGd_{1-x}(VO_4)$ observed from Fig. 3(a)–(d), should be mainly due to the Y doping as observed for Nd:$Y_xGd_{1-x}(VO_4)$. The wavenumbers of yYb:$Y_xGd_{1-x}VO_4$ as a function of Y content are also listed in Table 1, where we observe that most of the observed wavenumbers in the system y(Nd,Yb):$Y_xGd_{1-x}(VO_4)$ exhibit a one-phonon-like behavior, as expected for *RE*VO_4 compounds with zircon-type structure.

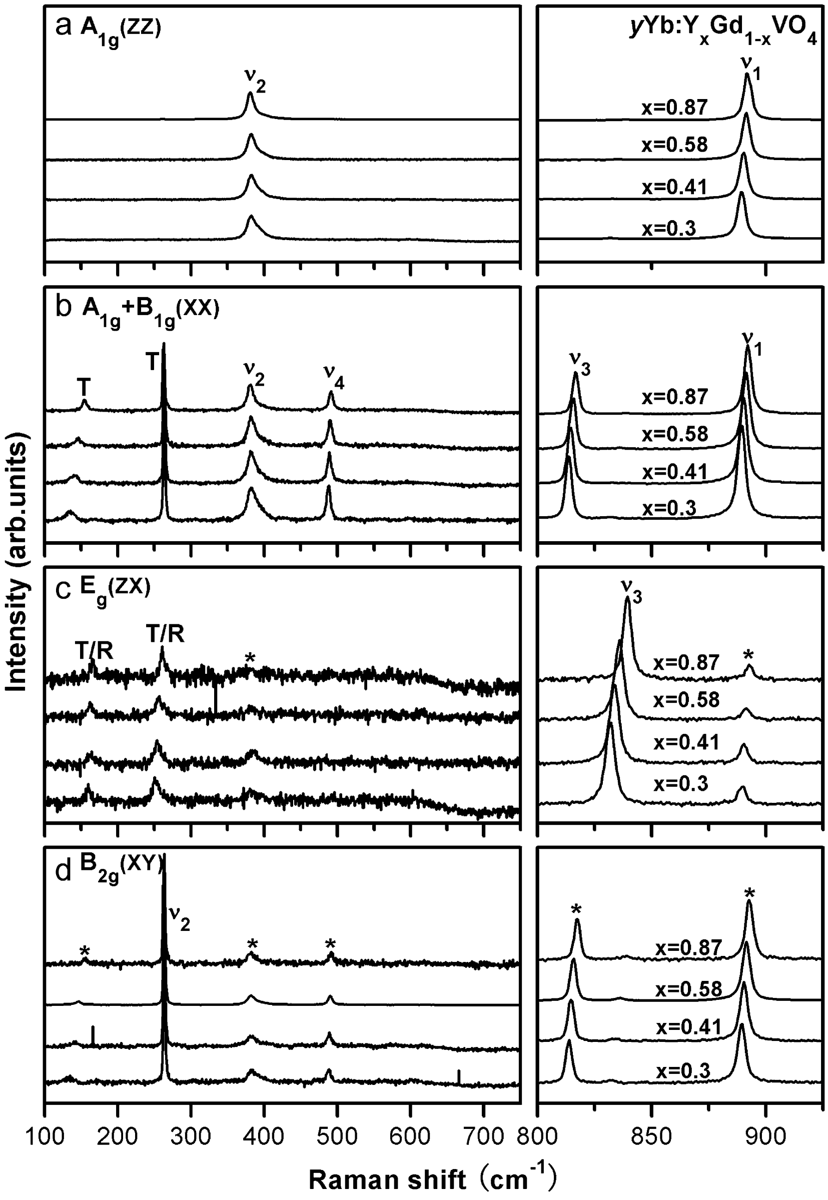

Fig. 3. Room temperature polarized Raman spectrum of yYb:$Y_xGd_{1-x}VO_4$, with $(y,x)=(0.0048, 0.3)$, (0.0071, 0.41), (0.0092, 0.58), (0.0135, 0.87), (0.008, 1), recorded in different polarizations: (a) (*zz*), (b) (*xx*), (c) (*zx*), and (d) (*xy*).

4. Conclusion

We investigated the changes in the phonon spectra of mixed (Nd,Yb):$Y_xGd_{1-x}(VO_4)$ crystals at room temperature. The phonon symmetry assignment was given and the observed wavenumbers were correlated with x to establish systematic variations. For Yb:$GdVO_4$, neither broadening nor wavenumber shifting of the modes were observed, indicating that Yb doping up to 0.035 produces no significant modification of the $GdVO_4$ structure. For Nd:$Y_xGd_{1-x}(VO_4)$ and yYb:$Y_xGd_{1-x}(VO_4)$ we observed that the wavenumber of most of the modes increases with increasing x; irrespective of Nd and Yb levels considered. This one-phonon-like behavior is due to the lattice contraction when Gd is replaced by Y. As these materials can be used in quantum electronics, the understanding of disordering should be taken into account when interpreting their optical and laser properties.

Acknowledgments

Financial support from the Brazilian agencies CNPq, CAPES, and FUNCAP is gratefully acknowledged. The work at Shandong University is supported by the program of Introducing Talents of Discipline to Universities in China (111 program).

References

[1] C.P. Wyss, W. Luthy, H.P. Weber, V.I. Vlasov, Y.D. Zavartsev, P.A. Studenikin, A.I. Zagumennyi, I.A. Shcherbakov, Appl. Phys. B 68 (1999) 659–661.
[2] H.J. Zhang, X.L. Meng, L. Zhu, J.H. Liu, C.Q. Wang, Z.S. Shao, J. Jpn., Appl. Phys. Part 2—Letters 38 (1999) L1231–L1233.
[3] C.Q. Wang, Y.T. Chow, L. Reekie, W.A. Gambling, H.J. Zhang, L. Zhu, X.L. Meng, Appl. Phys. B 70 (2000) 769–772.
[4] H.J. Zhang, X.L. Meng, J.H. Liu, L. Zhu, C.Q. Wang, Z.S. Shao, J.Y. Wang, Y.G. Liu, J. Crystal Growth 216 (2000) 367–371.
[5] L.J. Qin, X.L. Meng, C.L. Du, Z.S. Shao, L. Zhu, B.C. Xu, H.J. Zhang, J. Jpn., Appl. Phys. Part 1—Regular Papers Short Notes & Review Papers 41 (2002) 6018–6019.
[6] H.J. Zhang, J.Y. Wang, C.Q. Wang, L. Zhu, X.B. Hu, X.L. Meng, M.H. Jiang, Opt. Mater. 23 (2003) 449–454.
[7] H. Luo, D.Y. Tang, G.Q. Xie, H.J. Zhang, L.J. Qin, H.H. Yu, L.Y. Ng, L.J. Qian, Opt. Commun. 281 (2008) 5382–5384.
[8] J. Liu, W. Han, H. Zhang, H. Yang, V. Petrov, Appl. Phys. B 98 (2010) 87–91.
[9] H.J. Zhang, J.H. Liu, J.Y. Wang, C.Q. Wang, L. Zhu, Z.S. Shao, X.L. Meng, X.B. Hu, Y.T. Chow, M.H. Jiang, Opt. Lasers Eng. 38 (2002) 527–536.
[10] J. Liu, Y. Wan, W. Han, H. Yang, H. Zhang, J. Wang, Appl. Phys. B 98 (2010) 69–76.
[11] J.H. Liu, H.J. Zhang, X. Mateos, W.J. Han, V. Petrov, J.Y. Wang, Opt. Exps. 16 (2008) 17729–17734.
[12] S.P. Ng, D.Y. Tang, A.Q. Liu, L.J. Qin, X.L. Meng, Opt. Commun. 259 (2006) 256–260.
[13] J.L. He, Y.X. Fan, J. Du, Y.G. Wang, S. Liu, H.T. Wang, L.H. Zhang, Y. Hang, Opt. Lett. 29 (2004) 2803–2805.
[14] J.H. Liu, Z.P. Wang, X.L. Meng, Z.S. Shao, B. Ozygus, A. Ding, H. Weber, Opt. Lett. 28 (2003) 2330–2332.
[15] H.H. Yu, H.J. Zhang, Z.P. Wang, J.Y. Wang, Y.G. Yu, Z.S. Shao, M.H. Jiang, X.Y. Zhang, Appl. Phys. Lett. 90 (2007) 113109.
[16] A.D. Nguyen, K. Murdoch, N. Edelstein, L.A. Boatner, M.M. Abraham, Phys. Rev. B 56 (1997) 7974–7987.
[17] R.T. Harley, W. Hayes, S.R.P. Smith, Solid State Commun. 9 (1971) 515–517.
[18] I. Guedes, Y. Hirano, M. Grimsditch, N. Wakabayashi, C.K. Loong, L.A. Boatner, J. Appl. Phys. 90 (2001) 1843–1846.
[19] E.J. Baran, M.E. Escobar, L.L. Fournier, R.R. Filgueira, Z. Fur Anorganische Und Allgemeine Chemie 472 (1981) 193–199.
[20] M.E. Escobar, E.J. Baran, Z. Naturforsch. a—J. Phys. Sci. 35 (1980) 1110–1111.
[21] U.O. Krasovec, B. Orel, A. Surca, N. Bukovec, R. Reisfeld, Solid State Ionics 118 (1999) 195–214.
[22] B.P. Barbero, L.E. Cadus, Appl. Catalysis a—General 252 (2003) 133–147.
[23] C.-T. Au, W.-D. Zhang, J. Chem., Soc. Faraday Trans. 93 (1997) 1195–1204.
[24] C.C. Santos, E.N. Silva, A.P. Ayala, I. Guedes, P.S. Pizani, C.K. Loong, L.A. Boatner, J. Appl. Phys. 101 (2007) 053511.
[25] Y.G. Yu, J.Y. Wang, H.J. Zhang, H.H. Yu, Z.P. Wang, M.H. Jiang, H.R. Xia, R.I. Boughton, J. Opt. Soc. Am. B 25 (2008) 995–1001.
[26] L.J. Qin, X.L. Meng, C.L. Du, L. Zhu, B.C. Xu, Z.S. Shao, Z.Q. Liu, Q. Fang, R.F. Cheng, J. Alloys Compd. 354 (2003) 259–262.
[27] L.J. Qin, X.L. Meng, L. Zhu, J.H. Liu, B.C. Xu, H.Z. Xu, F.Y. Jiang, C.L. Du, X.Q. Wang, Z.S. Shao, Chem. Phys. Lett. 380 (2003) 273–278.
[28] D.L. Rousseau, R.P. Bauman, S.P.S. Porto, J. Raman Spectrosc. 10 (1981) 253–290.
[29] U. Kolitsch, D. Holstam, Eur. J. Mineral 16 (2004) 117–126.
[30] J. Isasi, M.L. Veiga, Y. Laureiro, R. Saezpuche, C. Pico, J. Alloys Compd. 177 (1991) 143–147.
[31] G.W. Lu, C.X. Li, W.C. Wang, Z.H. Wang, H.R. Xia, P. Zhao, Mater. Sci. Eng. B 98 (2003) 156–160.
[32] Y. Voron'ko, A. Sobol, V. Shukshin, A. Zagumennyĭ, Y. Zavartsev, S. Kutovoĭ, Phys. Solid State 51 (2009) 1886–1893.
[33] M.R. Moura, A.P. Ayala, I. Guedes, M. Grimsditch, C.K. Loong, L.A. Boatner, J. Appl. Phys. 95 (2004) 1148–1151.
[34] J.C. Nipko, C.K. Loong, M. Loewenhaupt, M. Braden, W. Reichardt, L.A. Boatner, Phys. Rev. B 56 (1997) 11584–11592.
[35] S.A. Miller, H.H. Caspers, H.E. Rast, Phys. Rev. 168 (1968) 964–969.
[36] G.M. Begun, G.W. Beall, L.A. Boatner, W.J. Gregor, J. Raman Spectrosc. 11 (1981) 273–278.
[37] G.W. Beall, L.A. Boatner, D.F. Mullica, W.O. Milligan, J. Inorg., Nucl. Chem. 43 (1981) 101–105.
[38] D.F. Mullica, D.A. Grossie, L.A. Boatner, J. Solid State Chem. 58 (1985) 71–77.
[39] D.F. Mullica, D.A. Grossie, L.A. Boatner, Inorg. Chim. a—F-Block 109 (1985) 105–110.
[40] D.F. Mullica, W.O. Milligan, D.A. Grossie, G.W. Beall, L.A. Boatner, Inorg. Chim. a-F-Block 95 (1984) 231–236.
[41] Y.X. Ni, J.M. Hughes, A.N. Mariano, Am. Mineral 80 (1995) 21–26.
[42] H.Y. Li, S.Y. Zhang, S.H. Zhou, X.Q. Cao, Inorg. Chem. 48 (2009) 4542–4548.
[43] D.F. Mullica, E.L. Sappenfield, M.M. Abraham, B.C. Chakoumakos, L.A. Boatner, Inorg. Chim. Acta 248 (1996) 85–88.
[44] G. Lohmulle, G. Schmidt, B. Deppisch, V. Gramlich, C. Schering, Acta Crystallogr. B 29 (1973) 141–142.
[45] X.L. Hu, J.Z. Chen, N.F. Zhuang, J.L. Chen, J.M. Lan, F.T. Yang, J. Crystal Growth 256 (2003) 328–333.